This is a “preproof” accepted article for *Parasitology*.
This version may be subject to change during the production process.
10.1017/S0031182025000423

Characterization and microRNA quantification of plasma-derived extracellular vesicles in patients with *Plasmodium knowlesi* infection

Thunchanok Khammanee[1], Natakorn Nokchan[2], Piyatida Molika[2], Hansuk Buncherd[3], Kanitta Srinoun[3], Natta Tansila[3], Charinrat Saechan[3], Rachanida Praparatana[3], Nongyao Sawangjaroen[1], Suwannee Jitueakul[4], Chatree Ratcha[5], Churat Weeraphan[6], Jisnuson Svasti[6], Raphatphorn Navakanitworakul[2*] and Supinya Thanapongpichat[3*]

[1] Division of Biological Science, Faculty of Science, Prince of Songkla university, Songkhla 90110, Thailand; [2] Department of Biomedical Sciences and Biomedical Engineering, Faculty of Medicine, Prince of Songkla University, Songkhla 90110, Thailand; [3] Faculty of Medical Technology, Prince of Songkla University, Songkhla 90110, Thailand; [4] Haematology Unit, Department of Medical Technology and Pathology, Suratthani Hospital, Surat Thani Province, 84000, Thailand; [5] Medical Technology Laboratory, Phanom Hospital, Phanom District, Surat Thani, 84250, Thailand; [6] Laboratory of Biochemistry, Chulabhorn Research Institute, Lak Si, Bangkok 10210, Thailand

Corresponding authors: Supinya Thanapongpichat, Email: supinya.th@psu.ac.th; Raphatphorn Navakanitworakul, Email: nraphatp@medicine.psu.ac.th

*These authors contributed equally as co-corresponding authors.

https://doi.org/10.1017/S0031182025000423 Published online by Cambridge University Press

Abstract

MicroRNAs (miRNAs), derived from extracellular vesicles (EVs) are circulating intercellular communicators which influence pathogenesis and could be used as potential diagnostic markers. In this study, plasma-derived EVs from *Plasmodium knowlesi* infected patients (n=13) and healthy individuals (n=10) were isolated using size exclusion chromatography and ultracentrifugation. The presence of EVs was confirmed by transmission electron microscopy, Western immunoblotting, and quantified by nanoparticle tracking analysis. The extracellular vesicles isolated from patients exhibited a larger size, accompanied by an elevated concentration of EVs. The relative expression levels of eight human miRNAs were quantified using RT-qPCR. Compared to uninfected groups, hsa-miR-223-5p (p-value=0.0002) and hsa-miR-486-5p (p-value=0.025) were upregulated in *P. knowlesi* infected patients. Bioinformatic analysis revealed that these miRNAs are predicted to target both human host and parasite genes, and they were found to be enriched in various malaria-related pathways. The areas under the ROCs of hsa-miR-223-5p and hsa-miR-486-5p were 0.9154 and 0.8231, respectively suggesting the potential of EV-miRNAs as diagnostic markers. Results revealed that EV-miRNAs may play a significant role in the progression of *P. knowlesi* infection. Further investigations should explore their potential impact on gene expression regulation as diagnostic biomarkers or targets for therapeutic interventions.

Keywords: extracellular vesicle, microRNA, *P. knowlesi*, RT-qPCR, bioinformatic analysis

Introduction

Extracellular vesicles (EVs) are small lipid-bound vesicles that cells release either directly from the plasma membrane or through endosomal mechanisms, which merge with the membrane before entering the extracellular space (Théry *et al*., 2018). In the context of malaria infection, increased EV levels in the bloodstream have been observed to correlate with disease severity and clinical symptoms. These EVs, sourced from a variety of cells including infected erythrocytes, platelets, leukocytes, and endothelial cells are typically major contributors to malaria-derived EVs, with infected erythrocytes being a significant source (Sahu *et al*., 2013; Combes *et al*., 2004; Abels and Breakefield, 2016; Pankoui Mfonkeu *et al*., 2010). Platelets and reticulocytes play prominent roles in *P. vivax* infections as the main contributors to EV production (Toda *et al*., 2020). EVs play a significant role in the biological and pathogenic processes of malaria. EVs, originating from both host and parasite cells, transfer cell-specific biomolecules to immune cells or parasitized cells, influencing the inhibition or promotion of cytokine secretion, thereby inducing inflammation, promoting parasite survival, or facilitating gametocyte formation (Mantel *et al*., 2013; Regev-Rudzki *et al*., 2013; Sisquella *et al*., 2017).

MicroRNAs (miRNAs) are small non-coding RNA molecules that are secreted from cells into the bloodstream where they can either be bound to proteins or packaged into EVs. miRNAs participate in post-transcriptional gene regulation predominantly by binding to the 3' untranslated region (3'UTR) of the target mRNA, but they can also bind to the 5'UTR or even within the coding region of the mRNA, leading to protein translation inhibition or mRNA degradation (Schuster and Hsieh, 2019). *P. falciparum* is unable to produce miRNAs and lacks genes encoding Argonaute and Dicer (Xue *et al*., 2008). In this context, human miRNAs are involved in modulating gene expression in both *Plasmodium* parasites and human hosts, affecting the host immune response, inflammation, tissue damage, survival, and

https://doi.org/10.1017/S0031182025000423 Published online by Cambridge University Press

replication of the parasite throughout the life cycle (Lodde *et al*., 2022). In mild to severe malaria, the dysregulation of gene expression involved in immune regulation is marked by miRNAs such as miRNA-16, miRNA-155, miRNA-150, miRNA-223, and miRNA-451, indicating the potential of these miRNAs as biological markers for malaria infection (Rangel *et al*., 2020). Children with severe malaria showed increased expression of plasma miR-3158–3p, linked to seizures, and hsa-miR-4497, which is associated with parasite biomass and HRP2 levels. Both miRNAs are associated with acute respiratory distress syndrome (Gupta *et al*., 2020). In the serum of *P. vivax* infected patients, levels of miR-451 and miR-16 are decreased, while the level of miR-223 is not changed (Chamnanchanunt *et al*., 2015). The reduction was likely due to red blood cell degradation and miRNA clearance by the spleen. In *P. vivax* patients, other studies have demonstrated notably elevated plasma levels of miR-191, miR-223, miR-145, and miR-155 (Hadighi *et al*., 2022). An increase in miR-4454 and miR-7975 was also observed in patients with severe thrombocytopenia (Santos *et al*., 2021). Human miRNA has been found to be transferred to the intracellular parasite and regulate gene expression, with involvement in pathogenicity and host defense mechanisms (LaMonte *et al*., 2012; Dandewad *et al*., 2019). The overexpression of miR-451, miR-223, and let-7i in *P. falciparum* within sickle cell erythrocytes can regulate parasite genes, leading to a reduction in growth (LaMonte *et al*., 2012). *Plasmodium apicortin* targeted by miR-150-3p and miR-197-5p also impaired the growth and invasion of the malaria parasite (Chakrabarti *et al*., 2020). miRNAs found in both plasma and EVs are important diagnostic markers due to their stability in the bloodstream (Mantel *et al*., 2016). Notably, EV-derived miRNAs directly reflect the pathological characteristics of their cellular origin (Xu *et al*., 2022). EVs derived from *P. falciparum* cultures with infected red blood cells (iRBCs) showed high expression levels of specific small RNAs, while miR-451a, miR-486-5p, miR-92a-3p, miR-103a-3p, let-7b-5p, miR-181a, and miR-106b-5p were particularly prominent in the small RNA profile of

https://doi.org/10.1017/S0031182025000423 Published online by Cambridge University Press

these EVs (Mantel *et al*., 2016; Wang *et al*., 2017; Babatunde *et al*., 2018). *P. falciparum* EVs carrying miRNA-451 downregulate target genes (*CAV-1* and *ATF-2*) in endothelial cells, affecting vascular function (Mantel *et al*., 2016). Wang *et al*. demonstrated host-miRNA regulation, specifically showing that miR-451 and miR-140 from large EVs downregulate *VAR* genes encoding *P. falciparum* erythrocyte membrane protein (*PfEMP1*) (Wang *et al*., 2017). The expression of miRNA varies in different physiological conditions associated with the development of pathological diseases and organ damage. However, the expression of EV-derived miRNA from patient plasma in *Plasmodium knowlesi* malaria is not well studied.

P. knowlesi primarily resides in monkeys but can infect humans as a zoonotic disease transmitted through mosquito vectors. Infections caused by *P. knowlesi* range from asymptomatic cases to severe malaria, presenting with anemia, acute respiratory distress, renal failure, and thrombocytopenia, and can potentially be fatal. Its 24-hour intraerythrocytic cycle accelerates parasitemia and disease progression (Anstey *et al*., 2021), leading to severe outcomes or death if not promptly diagnosed and treated (Cox-Singh *et al*., 2010; Rajahram *et al*., 2012; Chantaramongkol and Buathong, 2016). In Thailand, *P. knowlesi* cases, once rare, have been steadily increasing. According to the Thai National Malaria Control Program, reported cases rose from 6 out of 11,595 in 2017 to 259 out of 16,680 in 2023 (ThaiMOPH, 2024).

The identification of EVs and miRNAs can help elucidate the molecular processes that contribute to these complications, potentially leading to better diagnostic tools and targeted interventions.

https://doi.org/10.1017/S0031182025000423 Published online by Cambridge University Press

Materials and methods

Blood sample collection and processing

Peripheral blood samples were obtained from individuals infected with the *P. knowlesi* parasite and from healthy donors. The blood specimens were obtained using leftover EDTA-containing tubes from the hospital in Southern Thailand. This study was approved by the Ethical Committee of the Faculty of Medicine at Prince of Songkla University (EC66-03). The characteristics of 13 *P. knowlesi* patients and 10 healthy donors are shown in Table 1. All *P. knowlesi* patients were confirmed by nested PCR (Putaporntip *et al*., 2011). The blood samples were centrifuged at 1,500 g for 10 minutes. The resulting plasma was then subjected to another round of centrifugation at 2,500 g for 15 minutes at 4°C, twice, to obtain platelet-free plasma. A 0.5-1 milliliter aliquot of the plasma supernatant was preserved at -80°C until further isolation of EVs.

EVs enrichment using size exclusion chromatography and ultracentrifugation

A commercial SEC (Size Exclusion Chromatography) qEV1/35 nm column from iZON Sciences (Christchurch, New Zealand) was used to isolate EVs from the plasma samples following the manufacturer's instructions (Figure 1A). The column was equipped with an automatic fraction collector. Before sample separation, the column was pre-equilibrated with PBS, which was previously filtered in a sterile manner through a 0.22 μm filter. For each isolation, 700 μl of plasma was loaded onto the top of the qEV column. Subsequently, four fractions (700 μl per fraction) were immediately collected into separate 1.5 ml microcentrifuge tubes. To further concentrate the EVs, the pooled fractions were subjected to ultracentrifugation at 120,000 g for 90 minutes. After centrifugation, the EV pellet was resuspended in PBS, resulting in a final volume of 100 μl.

https://doi.org/10.1017/S0031182025000423 Published online by Cambridge University Press

Transmission electron microscopy

The EVs were subjected to a fixing process using a 2.5% glutaraldehyde solution. Subsequently, these fixed EVs were carefully placed onto a Formvar carbon grid. To enhance visualization, the grids were treated with a 2% uranyl acetate stain and then allowed to dry at ambient temperature. Finally, the dried grids were observed and analyzed using an advanced Talos™ F200i transmission electron microscope manufactured by Thermo Scientific (MA, USA).

Western blot analysis

For immunoblotting analysis, 10 ug of isolated EVs were mixed with 5x loading buffer and then heated at 100°C for 5 minutes. Subsequently, the EV proteins were separated on a 12% polyacrylamide gel. Proteins were then transferred to polyvinylidene fluoride membranes. The membranes were blocked using 5% nonfat milk in TBS for 1 hour. After blocking, the membrane was washed three times with TBS-T (TBS with 0.1% Tween 20) for 10 minutes. The primary antibodies including anti-rabbit CD9 (Abcam ab223056) (Abcam, Cambridge, UK) at a dilution of 1:2,000 and anti-mouse GAPDH (Abcam ab8245) at a dilution of 1:20,000, were diluted in 1% nonfat milk in TBS-T and used as positive markers for EVs. The anti-cytochrome C1 (Biolegend, CA, USA) and anti-rabbit APOB (Abcam ab139401) were diluted at 1:1,000 as non-EV markers and indicators of lipoprotein contamination, respectively. The anti-mouse EXP-2 (The European Malaria Reagent Repository, Cat# 7.7) was diluted at 1:600 to detect against the parasitophorous vacuole membrane. After incubating with the primary antibodies, the PVDF membrane was washed three times with TBS-T buffer for 10 minutes. For secondary detection, secondary antibodies were applied at a dilution of 1:5,000 and incubated at room temperature for 1 hour. An ultra-sensitive enhanced chemiluminescent (ECL) HRP substrate was employed to visualize the specific

https://doi.org/10.1017/S0031182025000423 Published online by Cambridge University Press

proteins.

Quantification of extracellular vesicle

Nanoparticle tracking analysis (NTA) was employed to determine the size and concentration of the EVs. The NTA analyses were carried out using a NanoSight NS300 NTA 3.4 system equipped with a 488 nm laser. To conduct the analyses, aliquots of the isolated EVs were diluted 500-1,000-fold with 0.22 micron filtered deionized water, ensuring that the number of particles per frame fell within the range of 20-100. The camera level for each sample was set at 13, and the detection threshold was set at 5. The NTA software analyzed 5 videos for 60 seconds each in duplicate, while the temperature of the laser unit was maintained at 25°C. The obtained NTA data were compared for size distribution (mode) and concentration of particles between the *P. knowlesi* infection and healthy donor groups.

RNA extraction and reverse transcriptase quantitative PCR

The instructions provided by the manufacturer of an RNA extraction kit were followed to isolate total RNA. Initially, 350 µl of lysis buffer was added to the EV sample. The mixture was briefly vortexed and incubated for 5 minutes at room temperature. Next, 100% ethanol was added to the sample, and the resulting mixture was transferred to a spin column and centrifuged at 13,000 rpm for 1 minute. After washing, the isolated RNA was eluted from the spin column using 50 µl of elution buffer. The quantification of RNA was performed using a Nanodrop spectrophotometer. The complementary DNA was generated using a QuantiMir reverse transcription kit from System Biosciences (SBI). Subsequently, amplification was performed with specific miRNA primers, as detailed in Table 2. The amplification was carried out in a total volume of 20 µl PCR mixture which contained 10 µl of 2X qPCRBIO SyGreen Mix, 0.4 µM of each primer, and 1 µl of cDNA. The amplification thermal

condition consisted of 95°C for 1 minute followed by 40 cycles of 95°C for 15 s and 60°C for 1 minute. Each sample was analyzed in triplicate, with the negative control as nuclease-free water. Technical replicates with a standard deviation exceeding 0.5 were excluded and retested.

microRNA expression analysis

Quantification cycle (Cq) values were used to compare the relative quantities of miRNAs between the malarial and healthy samples. The Delta Cq (ΔCq) of the target miRNA was calculated by averaging triplicate values and subtracting them from the average Cq values of miR-451a in the corresponding samples. The hsa-mir451a-5p was used as a normalization control. ΔΔCq was then normalized by comparing the ΔCq of each sample to the mean ΔCq of the healthy control group. The expression of EV miRNA was assessed using the comparative Cq method ($-2^{\Delta\Delta Cq}$).

Target gene prediction and enrichment analysis

The target genes of upregulated miRNAs were predicted using TargetScan Release 8.0 (https://www.targetscan.org/vert_80/), miRDB (https://mirdb.org/), miRDIP (https://ophid.utoronto.ca/mirDIP/), and miRTarBase (https://mirtarbase.cuhk.edu.cn/). The human genes related to malaria infection were retrieved from the Kyoto Encyclopedia of Genes and Genomes (KEGG) malaria pathway. The candidate targets that overlapped between the miRNA target database and the malaria pathway in the KEGG database were selected using a Venn diagram. The Gene Ontology (GO) and KEGG enrichment analyses of individual miRNAs were conducted using the DIANA-miRPath v.4.0 (https://diana-lab.e-ce.uth.gr/app/miRPathv4) and DAVID gene annotation tool (https://david.ncifcrf.gov/). The prediction in DIANA-miRPath was based on experimentally supported targets from TarBase

8.0. The pathway union option was used, with false discovery rate (FDR) correction. The bar and bubble plots were generated using SRplot (https://www.bioinformatics.com.cn/srplot). The p-values were calculated by Fisher's exact test and the FDR was obtained by the Benjamini-Hochberg method. FDR values less than 0.05 were considered statistically significant for enrichment analysis. The DAVID online tool was conducted for upregulated miRNA, and p-value < 0.05 was set as a significant threshold.

The transcriptome data of *P. knowlesi* were retrieved from the PlasmoDB 8.0 database to determine the target binding of human miRNAs with *P. knowlesi* transcripts. Subsequently, an analysis of the selected miRNA sequences was conducted against the *P. knowlesi* strain H transcriptome using the psRNATarget tool (http://plantgrn.noble.org/psRNATarget/) with default recommended value of 5 (Dai *et al*., 2018).

Statistical analysis

All data were presented as the mean and standard error of the mean (SEM), with normality assessed using the D'Agostino-Pearson test. Student's t-test was used to assess differences in mode size and concentration of EVs between groups. The non-parametric Mann-Whitney U test was used to compare the expression levels of miRNAs between the plasma-derived EVs of healthy individuals and patients. This statistical analysis was conducted using GraphPad Prism software (version 9.0; GraphPad Software, San Diego, CA, USA). Receiver operating characteristic (ROC) curve analysis was performed to evaluate the diagnostic potential of miRNA expression levels for *P. knowlesi* infection. ROC curve analysis was carried out using delta Ct values (Canatan *et al*., 2022). The accuracy of the test was assessed by measuring the area under the ROC curve (AUC), which identified optimal sensitivity and specificity levels for distinguishing normal individuals from patients.

Results

Characterization of plasma-derived extracellular vesicles

TEM and Western blot analysis were used for EV characterization to evaluate the presence of the EVs isolated through SEC and UC-based methods (Figure 1A). TEM revealed spherical phospholipid bilayer structures with an approximate diameter of 100 nm (Figure 1B). As shown in Figure 1C, EVs demonstrated enrichment of exosomal protein markers including CD9 and glyceraldehyde-3-phosphate dehydrogenase (GAPDH), while Cytochrome C1 (CYC1) (non-EV marker) was not detected. The presence of parasite proteins EXP-2 was determined in EVs from *P. knowlesi* malaria patients. A signal for ApoB lipoprotein found in chylomicrons VLDL, IDL, and LDL particles was observed.

Quantification of extracellular vesicles size and concentration

The size and concentration distribution for each biological replicate were determined through NanoSight analysis. The particles displayed diameters ranging from under 50 nm to 600 nm, with most falling within the 50-100 nm size category. The 250-600 nm size range accounted for less than 1% of the total, indicating the presence of aggregated vesicles. The average modal size of isolated EVs from *P. knowlesi* infected individuals (*Pk*-EVs) was 81.9±1.75 nm, which was significantly larger than those from healthy donors (h-EVs) at 75.9±1.25 nm (p-value = 0.019) (Figure 1D). The size was consistent with the results of TEM. Larger EVs observed by the nanoparticle tracking system were possibly the result of aggregate formation. A statistically significant 2.4-fold increase in particle concentration was recorded for *P. knowlesi* infected patients, measuring 7.64×10^{10} particles/ml (range: 4.21×10^{10}-1.15×10^{11} particles/ml) compared to healthy donors, with concentration 3.24×10^{10} particles/ml (range: 1.15×10^{10}-5.56×10^{10} particles/ml), p-value < 0.0001 (Figure 1E). The size versus

https://doi.org/10.1017/S0031182025000423 Published online by Cambridge University Press

concentration of the two groups is illustrated in Figure 1F. The mean concentration of extracellular particles within the 1-50 nm size range was higher in healthy donors compared to those with *P. knowlesi* infection (8.32×10^{8} vs. 7.2×10^{8}). In the peak graph showing the 50-100 nm size range, the *P. knowlesi* infection group exhibited a significantly higher concentration at 6.03×10^{10} particles/ml, in contrast to 2.35×10^{10} particles/ml in healthy donors.

Relative expression of microRNAs

The SYBR Green qPCR-based detection methods were used to evaluate the expression of eight specific human miRNAs. The average Cq, ΔCq and $2^{-\Delta\Delta Cq}$ values for all miRNAs were calculated (Table 2 and Table 3), with hsa-miR-451a-5p serving as the endogenous control for data normalization. The relative expression of EV-miRNAs in malaria compared to healthy donors is shown in Figure 2. The qRT-PCR results revealed a significant increase in levels of hsa-miR-223-5p (p-value = 0.0002) and hsa-miR-486-5p (p-value =0.008) in *Pk*-EVs group. The other six miRNAs showed no significant differences in expression levels between *P. knowlesi* infection and healthy individual groups.

microRNA target prediction, GO and KEGG enrichment analysis

Prediction of the human-host gene targets for hsa-miRNA-223-5p and hsa-miRNA-486-5p, utilized information from four databases. Results showed that eight and one computationally predicted target were identified for hsa-miR-223-5p and hsa-miR-486-5p, respectively (Table 4). Intriguingly, CD40 was a shared target gene for both miRNAs. A pathway analysis of individual miRNAs was conducted using DIANA miRPath. Notably, no enriched pathways associated with hsa-miRNA-223-5p were observed in this analysis. By contrast, hsa-miRNA-486-5p showed enrichment in GO terms related to protein binding for molecular function

https://doi.org/10.1017/S0031182025000423 Published online by Cambridge University Press

(MF); cytosol, cytoplasm, and ribonucleoprotein complex for cellular component (CC) (Figure 3A), demonstrating significant enrichment in the KEGG pathways of the EGFR (Epidermal Growth Factor Receptor) tyrosine kinase inhibitor resistance pathway. DAVID was employed to determine overrepresented GO terms and KEGG pathways associated with hsa-miRNA-223-5p. This tool conducted functional and pathway enrichment analysis based on the predicted target genes of hsa-miRNA-223-5p. The top 10 ranked GO terms and KEGG pathways are displayed in Figure 3B and C, respectively. For GO BP, the predicted target genes were significantly enriched in phagocytosis, cellular response to mechanism stimulus, and positive regulation of NF-κB transcription factor activity, while for GO CC, the enriched GO terms were cell surface, an integral component of plasma membrane, and plasma membrane. In the KEGG pathway analysis, several predicted target genes were enriched in malaria, African trypanosomiasis, and NF-κB signaling pathway.

To explore potential interactions between miRNAs and *P. knowlesi* mRNAs and identify the potential gene targets of miRNAs in *P. knowlesi* mRNAs, the computational prediction software for miRNA-mRNA interactions, psRNATarget, was used. A total of 35 and 15 target candidates, with expectation values higher than 4.5, were identified as targets for hsa-miRNA-223-5p and hsa-miRNA-486-5p, respectively, as presented in Tables 5 and 6. Both miRNAs were shown to downregulate various genes in *P. knowlesi* by cleaving mRNA or translation inhibition.

Potential of extracellular vesicles-derived microRNAs as diagnostic markers

The area under the ROC curve analysis was performed to investigate the possibility of miRNA-223-5p and miRNA-486-5p as potential diagnostic biomarkers. ROC curve illustrates the plot between true positive rate (sensitivity) and false positive rate (100-specificity). The optimal cut-off was identified as the maximum likelihood ratio, computed as

sensitivity divided by (100 - specificity). The AUC was used to distinguish between the disease and healthy groups, where a value of 1 represents optimal discrimination. As shown in Figure 4, the AUC for miRNA-223-5p was 0.9154 (*p*-value=0.0008). At the relative expression level of miRNA-223-5p at the optimal cut-off value of 7.692, the sensitivity was 76.92% (95% CI: 49.74-91.82%), and the specificity was 90% (95% CI: 59.58-99.49%). For hsa-miRNA-486-5p, the AUC was determined to be 0.8231 (p-value=0.0092), with sensitivity and specificity 61.5% and 100%, respectively when the optimal cut-off value was 6.923.

Discussion

The investigation of exosomal miRNAs in samples from malaria patients is an expanding area of research that holds the potential to improve our understanding of malarial pathophysiology. The identification of miRNAs involved in the biology and pathology of *P. knowlesi* malaria has not been extensively studied. This study characterized plasma-derived EVs and presented quantitative data on miRNAs derived from EVs. Significant differences in plasma-derived EVs were noted between malaria patients and healthy individuals, with those from patients being both larger in size and more abundant. This increase in size may be associated with pathological changes in host cells due to cellular stress, such as membrane blebbing, alterations in cell morphology, and the formation of apoptotic bodies. These pathological changes can lead to the biogenesis and release of EVs of varying sizes, including larger subpopulations (Avalos-Padilla *et al*., 2021, Minwuyelet and Abiye 2022). Additionally, the immune response to *Plasmodium* infection may enhance EV production as part of the inflammatory response, resulting to an overall increase in both the quantity and size of EVs. The molecular mechanisms underlying the biogenesis of these different EV subpopulations may involve intracellular pathways such as endosomal sorting complexes

required for transport (ESCRT) (Opadokun and Rohrbach 2021, Minwuyelet and Abiye 2022). The increased levels of plasma EVs observed during malaria infections result from the activation of circulating cells, particularly in severe cases (Babatunde *et al*., 2020). However, our study had limited data regarding clinical symptoms, hematological information, or parasitemia, which hindered the understanding of their relationships with the level of EVs. In this study, the isolated EVs included those originating from *P. knowlesi* parasites expressing the EXP-2 protein, which are situated on the parasitophorous vacuole membrane (PVM) and are crucial for transporting proteins from the vacuole to the cytoplasm of red blood cells. These EVs may be internally generated and subsequently released externally, similar to the production of exosomes.

EV-miRNA quantification was performed using RT-qPCR targeting hsa-miR451-5p, hsa-miR150-5p, hsa-miR486-5p, hsa-miR15b-5p, hsa-miR16-5p, hsa-miR106b-5p, hsa-miR223-5p, let7a-5p, and let7b-5p. The hsa-miR451-5p was used as an endogenous control in our study due to its stable expression and relevance to the erythroid system. The miRNA-451a, which regulates erythroid differentiation and maturation, was found to be abundant in EVs under parasite culture conditions (Rathjen *et al*., 2006; Mantel *et al*., 2016; Wang *et al*., 2017). EVs from plasma of patients infected with *P. knowlesi* exhibited significantly higher levels of hsa-miR-223-5p and hsa-miR-486-5p compared to those from healthy individuals, while the others showed no significant differences between the two groups. Exosomal miRNA expression levels changes in response to varying conditions. Different isolation techniques can capture distinct EV subpopulations based on physical properties such as size and density. Consequently, the isolated EVs may represent different subpopulations, which can influence the miRNA and biomolecule profiles observed (Llorens-Revull *et al*., 2023). In a recent study that isolated EVs via ultracentrifugation, EV-derived miR-150-5p and miR-15b-5p were identified in patients infected with *P. vivax*. Furthermore, upregulation of let-7a-

5p was observed in both *P. vivax* and *P. falciparum* infections (Ketprasit *et al*., 2020). The miR-223 is involved in the proliferation and function of granulocytes and platelets (Fazi *et al*., 2005; Shi *et al*., 2015), implying that platelets and granulocytes might serve as potential sources of EVs during *P. knowlesi* infection. The upregulation of miR-223 in platelets is associated with increased platelet activation and aggregation (Gatsiou *et al*., 2012). During malaria infection, infected red blood cells could interact with platelets, leading to the release of chemokines and inflammatory cytokines (Srivastava and Srivastava, 2015). Hsa-miR-223 also forms complexes with lipoproteins circulating in the blood (Vickers *et al*., 2011). LDL has been observed interacting with the surface of EVs, making it interesting to determine whether this interaction is the result of contamination from the circulation. Isolating EVs from lipoproteins in the blood is still challenging due to the overwhelming abundance of lipoproteins, exceeding EVs by at least 10^5-fold (Zhang *et al*., 2020). SEC is effective in largely eliminating HDL, although LDL of comparable density might be co-isolated with EVs. Employing subsequent ultracentrifugation as a washing step can aid in minimizing contamination (Koster *et al*., 2021). miR-223 has been documented as being upregulated in sickle cell erythrocytes infected with *P. falciparum* (LaMonte *et al*., 2012) and in the plasma of *P. vivax* patients (Hadighi *et al*., 2022). Moreover, in mice with cerebral malaria, miR-223-3p, miR-19b-3p and miR-142-3p exhibited significant upregulation compared to noninfected mice (Martin-Alonso *et al*., 2018).

Computational target predictions were conducted for hsa-miR-223-5p and hsa-miR-486-5p on both human and malaria transcripts, along with an enrichment analysis in GO and KEGG pathways. The prediction indicated that hsa-miR223-5p targets several human transcripts including HGF, MET, VCAM-1, TLR4, MyD88, GYPA, GYPC and CD40. The HGF/MET signaling pathway plays a critical role in diverse cellular processes such as cell growth, survival, motility, and morphogenesis (Organ and Tsao, 2011). Moreover, it is essential for

the initial development of parasites within the host liver by preventing cell apoptosis and involving host-cell actin cytoskeleton reorganization (Carrolo *et al*., 2003). VCAM-1 contains six or seven immunoglobulin domains, is expressed on endothelial cells in blood vessels, and acts as a cell adhesion molecule (Cook-Mills *et al*., 2011). The elevated VCAM-1 expression is associated with the sequestration of *P. falciparum* in vessels, particularly in severe cases (Armah *et al*., 2005). TLR4 is expressed in immune cells including monocytes, macrophages, B cells, dendritic cells, and epithelial cells. Monocytes expressing TLR4 are activated by parasite-derived GPI anchors and hemozoin, leading to the production of proinflammatory cytokines. MyD88 acts as a key signaling protein, connecting the activated receptors with downstream signaling molecules. MyD88 activation leads to the activation of transcription factors such as NF-κB and MAPKs, which results in the production of proinflammatory cytokines like IL-1, TNF-α, and IL-6 (Dobbs, Crabtree, and Dent, 2020). GYPA and GYPC are cell surface receptors found on red blood cells that engage with parasite antigens such as EBA-175 and EBA-140, facilitating the invasion of parasites (Jaskiewicz *et al*., 2019). In this study, all predicted human host targets of hsa-miR-223-5p were found to be associated with specific biological processes and cellular components based on GO analysis. These targets are enriched in processes like phagocytosis, cellular response to mechanical stimuli, and NF-κB activation, which are critical for immune cell function and host defense. The enriched cellular components include the cell surface, integral components of the plasma membrane, and the plasma membrane, emphasizing the role of miR-223-5p in membrane-related immune interactions. Based on these findings, we hypothesized that miR-223-5p may target HGF, which acts as an anti-inflammatory mediator. If miR-223-5p reduces HGF levels, immune responses could shift toward a more proinflammatory state, thereby activating pathways such as NF-κB, TLR4, and MyD88 (Zhou *et al*., 2018). A previous study suggested a role for miRNAs in modulating inflammatory signaling pathways (Lee *et al*.,

https://doi.org/10.1017/S0031182025000423 Published online by Cambridge University Press

2021); however, direct evidence linking miR-223-5p to HGF suppression and subsequent activation of pro-inflammatory processes remains limited. Further experimental validation is needed to clarify whether miR-223-5p directly influences HGF-mediated immune modulation during *P. knowlesi* infection. Additionally, while miR-223-5p overexpression may help regulate inflammation and prevent tissue damage, it could also compromise the immune system's ability to clear the *Plasmodium* parasite, which utilizes various immune evasion strategies (Su *et al*., 2025). Moreover, it is important to note that hsa-miR-223-5p can exert varying effects on its target genes, depending on factors such as its subcellular location, expression level, the degree of complementarity with the target, and other regulatory elements in the cellular environment (O'Brien *et al*., 2018). Further investigation is needed to clarify its specific role in *P. knowlesi* infection.

Our results indicated an increase in hsa-miR-486-5p expression in plasma-derived EVs from *P. knowlesi* infected patients. This finding concurred with a previous study, wherein miRNA profiling of EVs isolated from *P. falciparum* culture revealed that hsa-miR-486-5p exhibited one of the highest expression levels (Babatunde *et al*., 2018). MiR-486-5p is expressed abundantly in RBCs and is involved in RBC maturation. CD40 was predicted as the target of miR-486-5p. CD40, a membrane glycoprotein, is prominently expressed in B lymphocytes, dendritic cells, monocytes, and platelets. CD40 expression is induced by proinflammatory factors and regulated by transcriptional factors including NF-κB, responsible for the inflammatory response (Antoniades *et al*., 2009). The results of this study demonstrated that miR-486-5p was enriched in protein binding and cytosol. Moreover, the parasite mRNA has been predicted as a target of human miR-223-5p, with the *SICAvar* gene being the most frequently identified target in the database. The *P. knowlesi* schizont infected cell agglutination (SICA) var gene family, expressed on the surface of infected erythrocytes, codes for antigenic variation, analogous to the virulence-associated PfEMP1 gene (Lapp *et*

al., 2013). The *SICAvar* gene is associated with cytoadhesion of *P. knowlesi* infected red blood cells with endothelial cells in the umbilical vein and the gastrointestinal tract (Peterson *et al*., 2022, Chuang *et al*., 2022). EVs are found to harbor promising miRNA candidates, serving as robust biomarkers with an AUC close to 1. This characteristic makes them valuable for diagnostic purposes. The resistance of miRNAs to degradation, facilitated by their protection within vesicles during circulation, adds to the appeal of exosome miRNAs as stable and reliable disease biomarkers. However, the sorting process of miRNAs in EVs is not well understood and may exhibit either selective or non-selective characteristics, potentially influenced by the subtypes of EVs (Temoche-Diaz *et al*., 2019). Recognition by RNA-binding proteins such as hnRNPA2B1 and Argonaute-2, specific structural features, post-transcriptional modifications of miRNA, and cellular content can contribute to the loading of miRNAs into EVs (Qiu *et al*., 2021). Our findings shed light on miRNAs associated with *P. knowlesi* infection, providing valuable insights into their molecular mechanisms. Further research is required to explore the role of miRNAs in malaria pathogenesis. In-depth *in vitro* and *in vivo* studies, along with investigations in human populations are required to confirm these findings and assess the potential of miRNAs as a therapeutic target or diagnostic marker.

Conclusions

This study established a foundation for understanding the pathophysiology of *P. knowlesi*, highlighting the increased expression of EV-miRNAs, specifically hsa-miR-223-5p and hsa-miR-486-5p, which could reflect the underlying processes of *P. knowlesi* infection. Further studies should validate the functionality of EV-miRNAs, as they have the potential to provide crucial insights to develop new diagnostic or patient monitoring biomarkers.

Funding statement. This research was supported by Prince of Songkla University (Grant No. MET6602031S and MET6402038S), National Science, Research and Innovation Fund (NSRF) and Prince of Songkla University (Grant No. MET6601206S), PSU Ph.D. Scholarship contract no. PSU_PHD2562-004 and the NSRF via the Program Management Unit for Human Resources & Institutional Development, Research and Innovation (Grant No. B13F660074).

Competing interests. The authors declare no competing interests.

Author contributions. Conceptualization: ST and RN, Software: TK and NN, Investigation: TK and PM. Resources: CW, JS, SJ, CR, and RN, Formal Analysis: HB, KS, NT, RP, CS, and NS, Writing – Original Draft Preparation: TK and ST, Writing – Revised Draft and Editing: ST, RN, HB, JS, and CW. All authors have read and approved the final version of the revised manuscript.

Ethical statement. All samples were obtained as leftover specimens from routine laboratory procedures. This study received ethical approval from the Ethics Committee of the Faculty of Medical Technology, Prince of Songkla University, under approval number EC66-03.

https://doi.org/10.1017/S0031182025000423 Published online by Cambridge University Press

References

Abels, E. R., & Breakefield, X. O. (2016). Introduction to Extracellular Vesicles: Biogenesis, RNA Cargo Selection, Content, Release, and Uptake. *Cellular and molecular neurobiology*, *36*(3), 301–312. https://doi.org/10.1007/s10571-016-0366-z

Anstey, N. M., Grigg, M. J., Rajahram, G. S., Cooper, D. J., William, T., Kho, S., & Barber, B. E. (2021). Knowlesi malaria: Human risk factors, clinical spectrum, and pathophysiology. *Advances in parasitology*, *113*, 1–43. https://doi.org/10.1016/bs.apar.2021.08.001

Antoniades, C., Bakogiannis, C., Tousoulis, D., Antonopoulos, A. S., & Stefanadis, C. (2009). The CD40/CD40 ligand system: linking inflammation with atherothrombosis. *Journal of the American College of Cardiology*, *54*(8), 669–677. https://doi.org/10.1016/j.jacc.2009.03.076

Armah, H., Wired, E. K., Dodoo, A. K., Adjei, A. A., Tettey, Y., & Gyasi, R. (2005). Cytokines and adhesion molecules expression in the brain in human cerebral malaria. *International journal of environmental research and public health*, *2*(1), 123–131. https://doi.org/10.3390/ijerph2005010123.

Avalos-Padilla, Y., Georgiev, V. N., Lantero, E., Pujals, S., Verhoef, R., N Borgheti-Cardoso, L., Albertazzi, L., Dimova, R., & Fernàndez-Busquets, X. (2021). The ESCRT-III machinery participates in the production of extracellular vesicles and protein export during *Plasmodium falciparum* infection. *PLoS pathogens*, *17*(4), e1009455. https://doi.org/10.1371/journal.ppat.1009455.

Babatunde, K. A., Mbagwu, S., Hernández-Castañeda, M. A., Adapa, S. R., Walch, M., Filgueira, L., Falquet, L., Jiang, R. H. Y., Ghiran, I., & Mantel, P. Y. (2018). Malaria infected red blood cells release small regulatory RNAs through extracellular vesicles. *Scientific reports*, *8*(1), 884. https://doi.org/10.1038/s41598-018-19149-9.

Babatunde, K. A., Yesodha Subramanian, B., Ahouidi, A. D., Martinez Murillo, P., Walch, M., & Mantel, P. Y. (2020). Role of Extracellular Vesicles in Cellular Cross Talk in Malaria. *Frontiers in immunology*, *11*, 22. https://doi.org/10.3389/fimmu.2020.00022.

Canatan, D., Yılmaz, O., Sonmez, Y., Cim, A., Baykara, M., Savas, M., Coskun, H. S., Goksu, S. S., & Aktekin, M. R. (2022). Use of MicroRNAs as biomarkers in the early diagnosis of prostate cancer. *Acta bio-medica : Atenei Parmensis*, *93*(3), e2022089. https://doi.org/10.23750/abm.v93i3.11642.

Carrolo, M., Giordano, S., Cabrita-Santos, L., Corso, S., Vigário, A. M., Silva, S., Leirião, P., Carapau, D., Armas-Portela, R., Comoglio, P. M., Rodriguez, A., & Mota, M. M. (2003). Hepatocyte growth factor and its receptor are required for malaria infection. *Nature medicine*, *9*(11), 1363–1369. https://doi.org/10.1038/nm947.

Chakrabarti, M., Garg, S., Rajagopal, A., Pati, S., & Singh, S. (2020). Targeted repression of *Plasmodium* apicortin by host microRNA impairs malaria parasite growth and invasion. *Disease models & mechanisms*, *13*(6), dmm042820. https://doi.org/10.1242/dmm.042820.

Chamnanchanunt, S., Kuroki, C., Desakorn, V., Enomoto, M., Thanachartwet, V., Sahassananda, D., Sattabongkot, J., Jenwithisuk, R., Fucharoen, S., Svasti, S., & Umemura, T. (2015). Downregulation of plasma miR-451 and miR-16 in *Plasmodium vivax* infection. *Experimental parasitology*, *155*, 19–25. https://doi.org/10.1016/j.exppara.2015.04.013.

Chantaramongkol, J., & Buathong, R. (2016). A fatal malaria caused by *Plasmodium knowlesi* infection in a healthy man, Betong, Yala, Thailand April, 2016. *International Journal of Infectious Diseases*, 53 : 124.

Chuang, H., Sakaguchi, M., Lucky, A. B., Yamagishi, J., Katakai, Y., Kawai, S., & Kaneko, O. (2022). SICA-mediated cytoadhesion of *Plasmodium knowlesi*-infected red

blood cells to human umbilical vein endothelial cells. *Scientific reports*, *12*(1), 14942. https://doi.org/10.1038/s41598-022-19199-0

Combes, V., Taylor, T. E., Juhan-Vague, I., Mège, J. L., Mwenechanya, J., Tembo, M., Grau, G. E., & Molyneux, M. E. (2004). Circulating endothelial microparticles in malawian children with severe falciparum malaria complicated with coma. *JAMA*, *291*(21), 2542–2544. https://doi.org/10.1001/jama.291.21.2542-b

Cook-Mills, J. M., Marchese, M. E., & Abdala-Valencia, H. (2011). Vascular cell adhesion molecule-1 expression and signaling during disease: regulation by reactive oxygen species and antioxidants. *Antioxidants & redox signaling*, *15*(6), 1607–1638. https://doi.org/10.1089/ars.2010.3522.

Cox-Singh, J., Hiu, J., Lucas, S. B., Divis, P. C., Zulkarnaen, M., Chandran, P., Wong, K. T., Adem, P., Zaki, S. R., Singh, B., & Krishna, S. (2010). Severe malaria - a case of fatal *Plasmodium knowlesi* infection with post-mortem findings: a case report. *Malaria journal*, *9*, 10. https://doi.org/10.1186/1475-2875-9-10.

Dandewad, V., Vindu, A., Joseph, J., & Seshadri, V. (2019). Import of human miRNA-RISC complex into *Plasmodium falciparum* and regulation of the parasite gene expression. *Journal of biosciences*, *44*(2), 50.

Dobbs, K. R., Crabtree, J. N., & Dent, A. E. (2020). Innate immunity to malaria-The role of monocytes. *Immunological reviews*, *293*(1), 8–24. https://doi.org/10.1111/imr.12830.

Fazi, F., Rosa, A., Fatica, A., Gelmetti, V., De Marchis, M. L., Nervi, C., & Bozzoni, I. (2005). A minicircuitry comprised of microRNA-223 and transcription factors NFI-A and C/EBPalpha regulates human granulopoiesis. *Cell*, *123*(5), 819–831. https://doi.org/10.1016/j.cell.2005.09.023.

Gatsiou, A., Boeckel, J. N., Randriamboavonjy, V., & Stellos, K. (2012). MicroRNAs in platelet biogenesis and function: implications in vascular homeostasis and

inflammation. *Current vascular pharmacology*, *10*(5), 524–531. https://doi.org/10.2174/157016112801784611.

Gupta, H., Rubio, M., Sitoe, A., Varo, R., Cisteró, P., Madrid, L., Cuamba, I., Jimenez, A., Martiáñez-Vendrell, X., Barrios, D., Pantano, L., Brimacombe, A., Bustamante, M., Bassat, Q., & Mayor, A. (2021). Plasma MicroRNA Profiling of *Plasmodium falciparum* Biomass and Association with Severity of Malaria Disease. *Emerging infectious diseases*, *27*(2), 430–442. https://doi.org/10.3201/eid2702.191795.

Hadighi, R., Heidari, A., Fallah, P., Keshavarz, H., Tavakoli, Z., Sholeh Mansouri, & Sadrkhanloo, M. (2022). Key plasma microRNAs variations in patients with *Plasmodium vivax* malaria in Iran. *Heliyon*, *8*(3), e09018. https://doi.org/10.1016/j.heliyon.2022.e09018.

Jaskiewicz, E., Jodłowska, M., Kaczmarek, R., & Zerka, A. (2019). Erythrocyte glycophorins as receptors for Plasmodium merozoites. *Parasites & vectors*, *12*(1), 317. https://doi.org/10.1186/s13071-019-3575-8.

Ketprasit, N., Cheng, I. S., Deutsch, F., Tran, N., Imwong, M., Combes, V., & Palasuwan, D. (2020). The characterization of extracellular vesicles-derived microRNAs in Thai malaria patients. *Malaria journal*, *19*(1), 285. https://doi.org/10.1186/s12936-020-03360-z.

Koster, H. J., Rojalin, T., Powell, A., Pham, D., Mizenko, R. R., Birkeland, A. C., & Carney, R. P. (2021). Surface enhanced Raman scattering of extracellular vesicles for cancer diagnostics despite isolation dependent lipoprotein contamination. *Nanoscale*, *13*(35), 14760–14776. https://doi.org/10.1039/d1nr03334d.

LaMonte, G., Philip, N., Reardon, J., Lacsina, J. R., Majoros, W., Chapman, L., Thornburg, C. D., Telen, M. J., Ohler, U., Nicchitta, C. V., Haystead, T., & Chi, J. T. (2012). Translocation of sickle cell erythrocyte microRNAs into *Plasmodium falciparum*

inhibits parasite translation and contributes to malaria resistance. *Cell host & microbe*, *12*(2), 187–199. https://doi.org/10.1016/j.chom.2012.06.007.

Lapp, S. A., Korir-Morrison, C., Jiang, J., Bai, Y., Corredor, V., & Galinski, M. R. (2013). Spleen-dependent regulation of antigenic variation in malaria parasites: *Plasmodium knowlesi* SICAvar expression profiles in splenic and asplenic hosts. *PloS one*, *8*(10), e78014. https://doi.org/10.1371/journal.pone.0078014.

Lee, L., Howitt, B., Cheng, T., King, M., Stawiski, K., Fendler, W., Chowdhury, D., Matulonis, U., & Konstantinopoulos, P. A. (2021). MicroRNA profiling in a case-control study of African American women with uterine serous carcinoma. *Gynecologic oncology*, *163*(3), 453–458.

Llorens-Revull, M., Martínez-González, B., Quer, J., Esteban, J. I., Núñez-Moreno, G., Mínguez, P., Burgui, I., Ramos-Ruíz, R., Soria, M. E., Rico, A., Riveiro-Barciela, M., Sauleda, S., Piron, M., Corrales, I., Borràs, F. E., Rodríguez-Frías, F., Rando, A., Ramírez-Serra, C., Camós, S., Domingo, E., … Costafreda, M. I. (2023). Comparison of Extracellular Vesicle Isolation Methods for miRNA Sequencing. *International journal of molecular sciences*, *24*(15), 12183. https://doi.org/10.3390/ijms241512183.

Lodde, V., Floris, M., Muroni, M. R., Cucca, F., & Idda, M. L. (2022). Non-coding RNAs in malaria infection. *Wiley interdisciplinary reviews. RNA*, *13*(3), e1697. https://doi.org/10.1002/wrna.1697.

Mantel, P. Y., Hjelmqvist, D., Walch, M., Kharoubi-Hess, S., Nilsson, S., Ravel, D., Ribeiro, M., Grüring, C., Ma, S., Padmanabhan, P., Trachtenberg, A., Ankarklev, J., Brancucci, N. M., Huttenhower, C., Duraisingh, M. T., Ghiran, I., Kuo, W. P., Filgueira, L., Martinelli, R., & Marti, M. (2016). Infected erythrocyte-derived extracellular vesicles alter vascular function via regulatory Ago2-miRNA complexes in malaria. *Nature communications*, *7*, 12727. https://doi.org/10.1038/ncomms12727.

Mantel, P. Y., Hoang, A. N., Goldowitz, I., Potashnikova, D., Hamza, B., Vorobjev, I., Ghiran, I., Toner, M., Irimia, D., Ivanov, A. R., Barteneva, N., & Marti, M. (2013). Malaria-infected erythrocyte-derived microvesicles mediate cellular communication within the parasite population and with the host immune system. *Cell host & microbe*, *13*(5), 521–534. https://doi.org/10.1016/j.chom.2013.04.009.

Martin-Alonso, A., Cohen, A., Quispe-Ricalde, M. A., Foronda, P., Benito, A., Berzosa, P., Valladares, B., & Grau, G. E. (2018). Differentially expressed microRNAs in experimental cerebral malaria and their involvement in endocytosis, adherens junctions, FoxO and TGF-β signalling pathways. *Scientific reports*, *8*(1), 11277. https://doi.org/10.1038/s41598-018-29721-y.

Minwuyelet, A., & Abiye, M. (2022) Role of Secretory Vesicles Derived from *Plasmodium* Infected Red Blood Cells to the Pathogenesis of Malaria: A Review. Adv Tech Biol Med. 10:360.

National Malaria Elimination Program. Malaria surveillance dashboard. Bangkok, Thailand: National Malaria Elimination Program, Department of Disease Control, Ministry of Public Health. 2024. https://malaria.ddc.moph.go.th/malariaR10/index_newversion.php. Accessed 31 Nov 2024.

Opadokun, T., & Rohrbach, P. (2021). Extracellular vesicles in malaria: an agglomeration of two decades of research. *Malaria journal*, *20*(1), 442. https://doi.org/10.1186/s12936-021-03969-8

Organ, S. L., & Tsao, M. S. (2011). An overview of the c-MET signaling pathway. *Therapeutic advances in medical oncology*, *3*(1 Suppl), S7–S19. https://doi.org/10.1177/1758834011422556.

Pankoui Mfonkeu, J. B., Gouado, I., Fotso Kuaté, H., Zambou, O., Amvam Zollo, P. H.,

Grau, G. E., & Combes, V. (2010). Elevated cell-specific microparticles are a biological marker for cerebral dysfunctions in human severe malaria. *PloS one*, *5*(10), e13415. https://doi.org/10.1371/journal.pone.0013415.

Peterson, M. S., Joyner, C. J., Lapp, S. A., Brady, J. A., Wood, J. S., Cabrera-Mora, M., Saney, C. L., Fonseca, L. L., Cheng, W. T., Jiang, J., Soderberg, S. R., Nural, M. V., Hankus, A., Machiah, D., Karpuzoglu, E., DeBarry, J. D., Tirouvanziam, R., Kissinger, J. C., Moreno, A., Gumber, S., … Galinski, M. R. (2022). *Plasmodium knowlesi* Cytoadhesion Involves SICA Variant Proteins. *Frontiers in cellular and infection microbiology*, *12*, 888496. https://doi.org/10.3389/fcimb.2022.888496.

Putaporntip, C., Buppan, P., & Jongwutiwes, S. (2011). Improved performance with saliva and urine as alternative DNA sources for malaria diagnosis by mitochondrial DNA-based PCR assays. *Clinical microbiology and infection : the official publication of the European Society of Clinical Microbiology and Infectious Diseases*, *17*(10), 1484–1491. https://doi.org/10.1111/j.1469-0691.2011.03507.x.

Qiu, Y., Li, P., Zhang, Z., & Wu, M. (2021). Insights Into Exosomal Non-Coding RNAs Sorting Mechanism and Clinical Application. *Frontiers in oncology*, *11*, 664904. https://doi.org/10.3389/fonc.2021.664904.

Rangel, G., Teerawattanapong, N., Chamnanchanunt, S., Umemura, T., Pinyachat, A., & Wanram, S. (2019). Candidate microRNAs as Biomarkers in Malaria Infection: A Systematic Review. *Current molecular medicine*, *20*(1), 36–43. https://doi.org/10.2174/1566524019666190820124827.

Rajahram, G. S., Barber, B. E., William, T., Menon, J., Anstey, N. M., & Yeo, T. W. (2012). Deaths due to *Plasmodium knowlesi* malaria in Sabah, Malaysia: association with reporting as Plasmodium malariae and delayed parenteral artesunate. *Malaria journal*, *11*, 284. https://doi.org/10.1186/1475-2875-11-284.

Rathjen, T., Nicol, C., McConkey, G., & Dalmay, T. (2006). Analysis of short RNAs in the malaria parasite and its red blood cell host. *FEBS letters*, *580*(22), 5185–5188. https://doi.org/10.1016/j.febslet.2006.08.063.

Regev-Rudzki, N., Wilson, D. W., Carvalho, T. G., Sisquella, X., Coleman, B. M., Rug, M., Bursac, D., Angrisano, F., Gee, M., Hill, A. F., Baum, J., & Cowman, A. F. (2013). Cell-cell communication between malaria-infected red blood cells via exosome-like vesicles. *Cell*, *153*(5), 1120–1133. https://doi.org/10.1016/j.cell.2013.04.029.

Sahu, U., Sahoo, P. K., Kar, S. K., Mohapatra, B. N., & Ranjit, M. (2013). Association of TNF level with production of circulating cellular microparticles during clinical manifestation of human cerebral malaria. *Human immunology*, *74*(6), 713–721. https://doi.org/10.1016/j.humimm.2013.02.006.

Santos, M. L. S., Coimbra, R. S., Sousa, T. N., Guimarães, L. F. F., Gomes, M. S., Amaral, L. R., Pereira, D. B., Fontes, C. J. F., Hawwari, I., Franklin, B. S., & Carvalho, L. H. (2021). The Interface Between Inflammatory Mediators and MicroRNAs in *Plasmodium vivax* Severe Thrombocytopenia. *Frontiers in cellular and infection microbiology*, *11*, 631333. https://doi.org/10.3389/fcimb.2021.631333

Shi, R., Zhou, X., Ji, W. J., Zhang, Y. Y., Ma, Y. Q., Zhang, J. Q., & Li, Y. M. (2015). The Emerging Role of miR-223 in Platelet Reactivity: Implications in Antiplatelet Therapy. *BioMed research international*, *2015*, 981841. https://doi.org/10.1155/2015/981841.

Srivastava., K, & Srivastava., K. (2015) Role of Platelet-Mediated Cytoadherence and Chemokines Release in Severe Malaria. *SOJ* Page 3 of 6 Immunol 3(3): 1-6. http://dx.doi.org/10.15226/soji/3/3/00132.

Su, X. Z., Xu, F., Stadler, R. V., Teklemichael, A. A., & Wu, J. (2025). Malaria: Factors affecting disease severity, immune evasion mechanisms, and reversal of immune

inhibition to enhance vaccine efficacy. *PLoS pathogens*, *21*(1), e1012853.

Temoche-Diaz, M. M., Shurtleff, M. J., Nottingham, R. M., Yao, J., Fadadu, R. P., Lambowitz, A. M., & Schekman, R. (2019). Distinct mechanisms of microRNA sorting into cancer cell-derived extracellular vesicle subtypes. *eLife*, *8*, e47544. https://doi.org/10.7554/eLife.47544.

Théry, C., Witwer, K. W., Aikawa, E., Alcaraz, M. J., Anderson, J. D., Andriantsitohaina, R., Antoniou, A., Arab, T., Archer, F., Atkin-Smith, G. K., Ayre, D. C., Bach, J. M., Bachurski, D., Baharvand, H., Balaj, L., Baldacchino, S., Bauer, N. N., Baxter, A. A., Bebawy, M., Beckham, C., … Zuba-Surma, E. K. (2018). Minimal information for studies of extracellular vesicles 2018 (MISEV2018): a position statement of the International Society for Extracellular Vesicles and update of the MISEV2014 guidelines. *Journal of extracellular vesicles*, *7*(1), 1535750. https://doi.org/10.1080/20013078.2018.1535750.

Toda, H., Diaz-Varela, M., Segui-Barber, J., Roobsoong, W., Baro, B., Garcia-Silva, S., Galiano, A., Gualdrón-López, M., Almeida, A. C. G., Brito, M. A. M., de Melo, G. C., Aparici-Herraiz, I., Castro-Cavadía, C., Monteiro, W. M., Borràs, E., Sabidó, E., Almeida, I. C., Chojnacki, J., Martinez-Picado, J., Calvo, M., … Del Portillo, H. A. (2020). Plasma-derived extracellular vesicles from *Plasmodium vivax* patients signal spleen fibroblasts via NF-kB facilitating parasite cytoadherence. *Nature communications*, *11*(1), 2761. https://doi.org/10.1038/s41467-020-16337-y.

Vickers, K. C., Palmisano, B. T., Shoucri, B. M., Shamburek, R. D., & Remaley, A. T. (2011). MicroRNAs are transported in plasma and delivered to recipient cells by high-density lipoproteins. *Nature cell biology*, *13*(4), 423–433. https://doi.org/10.1038/ncb2210.

Wang, Z., Xi, J., Hao, X., Deng, W., Liu, J., Wei, C., Gao, Y., Zhang, L., & Wang, H.

(2017). Red blood cells release microparticles containing human argonaute 2 and miRNAs to target genes of *Plasmodium falciparum*. *Emerging microbes & infections*, *6*(8), e75. https://doi.org/10.1038/emi.2017.63.

Xu, D., Di, K., Fan, B., Wu, J., Gu, X., Sun, Y., Khan, A., Li, P., & Li, Z. (2022). MicroRNAs in extracellular vesicles: Sorting mechanisms, diagnostic value, isolation, and detection technology. *Frontiers in bioengineering and biotechnology*, *10*, 948959. https://doi.org/10.3389/fbioe.2022.948959.

Xue, X., Zhang, Q., Huang, Y., Feng, L., & Pan, W. (2008). No miRNA were found in *Plasmodium* and the ones identified in erythrocytes could not be correlated with infection. *Malaria journal*, *7*, 47. https://doi.org/10.1186/1475-2875-7-47.

Zhang, X., Borg, E. G. F., Liaci, A. M., Vos, H. R., & Stoorvogel, W. (2020). A novel three step protocol to isolate extracellular vesicles from plasma or cell culture medium with both high yield and purity. *Journal of extracellular vesicles*, *9*(1), 1791450. https://doi.org/10.1080/20013078.2020.1791450.

Zhou, W., Pal, A. S., Hsu, A. Y., Gurol, T., Zhu, X., Wirbisky-Hershberger, S. E., Freeman, J. L., Kasinski, A. L., & Deng, Q. (2018). MicroRNA-223 Suppresses the Canonical NF-κB Pathway in Basal Keratinocytes to Dampen Neutrophilic Inflammation. *Cell reports*, *22*(7), 1810–1823.

https://doi.org/10.1017/S0031182025000423 Published online by Cambridge University Press

Table 1. Characteristics of the study subjects

Characteristic	*P. knowlesi* patient (n=13)	Healthy donor (n=10)	*p*-value
Sex, male (%)	53.85	40	0.6802 [a]
Age, years (mean± SD)	41.8±13.122	36±5.963	0.1107 [b]

[a:] Fisher's exact test
[b:] Mann-Whitney U test

https://doi.org/10.1017/S0031182025000423 Published online by Cambridge University Press

Table 2. miRNA sequences and Cq values

miRNA	miRbase accession number	Sequence (5'-3')	Mean Cq ±SEM	
			Uninfected	*P. knowlesi* infection
hsa-miR-451a	MIMAT0001631	AAACCGUUACCAUUACUGAGUU	27.22 ±0.55	28.08 ±0.25
hsa-miR-150-5p	MIMAT0000451	UCUCCCAACCCUUGUACCAGUG	27.53 ±0.55	28.52 ±0.44
hsa-miR-486-5p	MIMAT0002177	UCCUGUACUGAGCUGCCCCGAG	27.09 ±0.82	26.80 ±0.32
hsa-miR-15b-5p	MIMAT0000417	UAGCAGCACAUCAUGGUUUACA	28.82 ±0.46	30.61 ±0.47
hsa-miR-16-5p	MIMAT0000069	UAGCAGCACGUAAAUAUUGGCG	27.79 ±0.73	29.98 ±0.65
hsa-let-7a-5p	MIMAT0000062	UGAGGUAGUAGGUUGUAUAGUU	28.8 ±0.43	30.23 ±0.46
hsa-miR-223-5p	MIMAT0004570	CGUGUAUUUGACAAGCUGAGUU	29.48 ±0.48	28.52 ±0.31
hsa-let-7b-5p	MIMAT0000063	UGAGGUAGUAGGUUGUGUGGUU	30.31 ±0.15	30.9 ±0.25
hsa-miR-106b-5p	MIMAT0000680	UAAAGUGCUGACAGUGCAGAU	30.83 ±0.25	32.36 ±0.31

https://doi.org/10.1017/S0031182025000423 Published online by Cambridge University Press

Table 3. Evaluation of miRNA expression between healthy controls and patients

miRNA	Mean ΔCq ±SEM		Mean relative expression ($2^{-\Delta\Delta Cq}$) ±SEM		p-value
	Uninfected	*P. knowlesi* infected	Uninfected	*P. knowlesi* infected	
hsa-miR-150-5p	0.31 ±0.2	0.44 ±0.58	1.10 ±0.18	1.77 ±0.49	0.66
hsa-miR-486-5p	-0.13 ±0.31	-1.27 ±0.31	1.20 ±0.22	2.84 ±0.56	0.025
hsa-miR-15b-5p	1.6 ±0.32	2.53 ±0.5	1.27 ±0.33	0.95 ±0.28	0.343
hsa-miR-16-5p	0.57 ±0.28	1.9 ±0.7	1.16 ±0.18	1.42 ±0.67	0.166
hsa-let-7a-5p	1.58 ±0.39	2.15 ±0.59	1.33 ±0.31	1.24 ±0.3	0.648
hsa-miR-223-5p	2.05 ±0.44	0.44 ±0.15	1.29 ±0.24	3.27 ±0.26	0.0002
hsa-let-7b-5p	3.09 ±0.66	2.82 ±0.41	1.95 ±0.58	2.03 ±0.7	0.927
hsa-miR-106b-5p	3.61 ±0.5	4.28 ±0.35	1.66 ±0.54	0.89 ±0.22	0.313

https://doi.org/10.1017/S0031182025000423 Published online by Cambridge University Press

Table 4. Potential human target genes of hsa-miR-223-5p and hsa-miR-486-5p related malaria pathway

miRNA	Target transcript	Target prediction database
hsa-mir-223-5p	*HGF*	targetScan, miRDB
	MET	targetScan, miRDIP
	TLR4	targetScan
	MYD88	targetScan
	GYPA	targetScan
	GYPC	targetScan
	VCAM1	targetScan
	CD40	targetScan
hsa-mir-486-5p	*CD40*	miRDIP, mirTarBase

*****GYPC: glycophorin C, HGF: hepatocyte growth factor, CD40: cluster of differentiation 40, TLR4: toll-like receptor 4, GYPA: glycophorin A, MYD88: myeloid differentiation primary response protein 88, MET: MET Proto-Oncogene, Receptor Tyrosine Kinase, VCAM1: vascular cell adhesion molecule 1

https://doi.org/10.1017/S0031182025000423 Published online by Cambridge University Press

Table 5. Predicted *P. knowlesi* mRNA targets by miRNA-223-5p

Target description	miRNA start	miRNA end	Target start	Target end	Alignment	Inhibition	Expectation
Plasmodium protein, unknown function (PKNH_1202000)	1	22	10449	10470	.:::::.:::.. ::::::	Cleavage	4.5
DNA topoisomerase 2, putative (PKNH_0420100)	1	22	2304	2325	..:::: :::::...:::.:.	Cleavage	4.5
DNA replication licensing factor MCM5, putative (PKNH_1311800)	1	22	455	476	:: :.: .:::..::::::.	Cleavage	4.5
conserved Plasmodium protein, unknown function (PKNH_0114700)	1	22	9003	9024	...: ::.:::.::.::..:	Cleavage	4.5
ATP-dependent RNA helicase DHX36, putative (PKNH_1315300)	1	22	2391	2412	:. :..:::: ::::::..:	Cleavage	4.5
SICAvar, type I (PKNH_0940500)	1	22	2521	2542	..:.::: : ::.:.::::.:	Cleavage	4.5
myosin B, putative	1	22	1494	1515	.:: ::. ::: ::.::::::	Translation	4.5

https://doi.org/10.1017/S0031182025000423 Published online by Cambridge University Press

(PKNH_1029900)							
SICAvar, type I (fragment)	1	22	1534	1555	..:.: ::: ::.:.::::.:	Cleavage	4.5
(PKNH_0003300)							
RAP protein, putative	1	22	2514	2535	:: .:: ::.:::::::	Cleavage	4.5
(PKNH_1120900)							
ATP-dependent DNA helicase DDX3X, putative	1	22	2244	2265	::: : :::::::..:	Cleavage	4.5
(PKNH_0616200)							
conserved Plasmodium protein, unknown function	1	22	87	108	::: .::: :::.::..::	Translation	4.5
(PKNH_0821400)							

https://doi.org/10.1017/S0031182025000423 Published online by Cambridge University Press

Table 5. Predicted *P. knowlesi* mRNA targets by miRNA-223-5p (cont).

Target description	miRNA start	miRNA end	Target start	Target end	Alignment	Inhibition	Expectation
isoleucine--tRNA ligase, putative (PKNH_1444500)	1	22	1035	1055	.: ::.: ::::::::: :::	Cleavage	4.5
DNA replication licensing factor MCM2, putative (PKNH_1340200)	1	22	2315	2336	::: :::::::::.::...:	Cleavage	5.0
deoxyribodipyrimidine photo-lyase, putative (PKNH_1019500)	1	22	1877	1898	:.:::::: :::: :: ::..:	Cleavage	5.0
nucleolar protein Nop52, putative (PKNH_0729800)	1	22	1714	1735	::. ::.::::::::: ::::	Cleavage	5.0
conserved Plasmodium protein, unknown function (PKNH_0412800)	1	22	596	618	: :.:::::::: :::::::::	Cleavage	5.0
D-tyrosyl-tRNA(Tyr) deacylase, putative (PKNH_0905800)	1	22	12	33	:.:::::: :::.::: :..:	Cleavage	5.0
conserved Plasmodium protein, unknown function	1	22	854	875	:::::.:::::::::. :	Cleavage	5.0

https://doi.org/10.1017/S0031182025000423 Published online by Cambridge University Press

(PKNH_1127500)							
SICAvar, type I (PKNH_1306200)	1	22	1426	1446	::: :: :::: :::::.::::	Translation	5.0
GAF domain-related protein, putative (PKNH_0409800)	1	22	159	181	.: ::::: :::::. :.::::::	Cleavage	5.0
conserved Plasmodium protein, unknown function (PKNH_0703500)	1	22	698	719	::::::: .:::::.:.:	Translation	5.0

https://doi.org/10.1017/S0031182025000423 Published online by Cambridge University Press

Table 5. Predicted *P. knowlesi* mRNA targets by miRNA-223-5p (cont).

Target description	miRNA start	miRNA end	Target start	Target end	Alignment	Inhibition	Expectation
dihydrouridine synthase, putative (PKNH_0716800)	1	22	1286	1307	:::::: ::::.:.::.	Cleavage	5.0
exported serine/threonine protein kinase, putative (PKNH_0313100)	1	22	4348	4369	: :::: :::::::::. ::	Cleavage	5.0
conserved Plasmodium protein, unknown function (PKNH_0722600)	1	22	1890	1911	: ::. :::.:::.....:	Cleavage	5.0
casein kinase 2, alpha subunit, putative (PKNH_0906000)	1	22	729	750	::::::::::::: ..:	Cleavage	5.0
conserved protein, unknown function (PKNH_1004400)	1	22	1374	1395	.: : .::::::::::::	Cleavage	5.0
adenylyl cyclase beta, putative (PKNH_0116300)	1	22	2922	2943	:..:.:: :.::.:.::.:	Cleavage	5.0
exoribonuclease, putative	1	22	2931	2952	::::::: :.::. :.:.:	Cleavage	5.0

https://doi.org/10.1017/S0031182025000423 Published online by Cambridge University Press

(PKNH_0707400)							
zinc finger protein, putative	1	22	1785	1806	:: .: :::: ::::::..:	Translation	5.0
(PKNH_1308700)							
conserved Plasmodium protein, unknown function	1	22	977	998	: .::: .:::.:: :: :::	Cleavage	5.0
(PKNH_1322200)							
palmitoyltransferase DHHC11, putative	1	22	551	572	::.: : :::..:::::.	Cleavage	5.0
(PKNH_0405000)							

https://doi.org/10.1017/S0031182025000423 Published online by Cambridge University Press

Table 5. Predicted *P. knowlesi* mRNA targets by miRNA-223-5p (cont).

Target description	miRNA start	miRNA end	Target start	Target end	Alignment	Inhibition	Expectation
Plasmodium exported protein, unknown function (PKNH_1401200)	1	22	1959	1980	.::: ::: : ::::::::	Translation	5.0
conserved Plasmodium protein, unknown function (PKNH_1138300)	1	22	6674	6695	::: ::: ::::::::.:	Translation	5.0
conserved Plasmodium protein, unknown function (PKNH_1350500)	1	22	5901	5922	.: .::::::::::.:.:	Cleavage	5.0
conserved Plasmodium protein, unknown function (PKNH_0506800)	1	22	3891	3912	: :.: .:: :.:::::::::	Cleavage	5.0

https://doi.org/10.1017/S0031182025000423 Published online by Cambridge University Press

Table 6. Predicted *P. knowlesi* mRNA targets by miRNA-486-5p

Target description	miRNA start	miRNA end	Target start	Target end	Alignment	Inhibition	Expectation
conserved Plasmodium protein, unknown function (PKNH_0946100)	1	22	5405	5426	::::::: .:.:: ::.:::.	Cleavage	4.5
conserved Plasmodium protein, unknown function (PKNH_0946100)	1	22	5672	5693	: :::.. .:: ::::::::	Cleavage	4.5
conserved Plasmodium protein, unknown function (PKNH_0718600)	1	22	894	914	::::::::.:: ::.:::.	Cleavage	4.5
cyclin-dependent kinases regulatory subunit, putative (PKNH_0207700)	1	22	1870	1891	: ::.::.:::: ::.::.	Cleavage	4.5
STAG domain-containing protein, putative (PKNH_1225300)	1	22	5318	5339	::: :::::::: .::: :	Cleavage	4.5
conserved Plasmodium protein, unknown function (PKNH_0718400)	1	22	4173	4194	:: : : :::::::.:::.	Cleavage	4.5
conserved Plasmodium protein, unknown function	1	22	2861	2882	.:: :.::::.. :::::::	Cleavage	5.0

https://doi.org/10.1017/S0031182025000423 Published online by Cambridge University Press

(PKNH_1419000)							
conserved Plasmodium protein, unknown function	1	22	3582	3603	::::: :: :.: ::.::::	Cleavage	5.0
(PKNH_1131100)							
dynein, putative	1	22	8085	8105	::: :: .::::::.::::	Cleavage	5.0
(PKNH_0610000)							
ATP-dependent DNA helicase DDX3X, putative	1	22	826	847	::::: :::::..:::	Cleavage	5.0
(PKNH_0616200)							

https://doi.org/10.1017/S0031182025000423 Published online by Cambridge University Press

Table 6. Predicted *P. knowlesi* mRNA targets by miRNA-486-5p (cont).

Target description	miRNA start	miRNA end	Target start	Target end	Alignment	Inhibition	Expectation
proteasome subunit beta type-7, putative (PKNH_1200500)	1	22	532	553	:: :::: ::::::::	Translation	5.0
conserved Plasmodium protein, unknown function (PKNH_1242300)	1	22	29	50	:: :.:::::. ::::: :	Cleavage	5.0
lysine-specific histone demethylase 1, putative (PKNH_1311700)	1	22	3760	3781	:: ::::.:::: : .:::	Cleavage	5.0
lysine-specific histone demethylase 1, putative (PKNH_0310700)	1	22	2758	2779	.: ::. :. :::::.:::	Translation	5.0
S-adenosylmethionine synthetase, putative (PKNH_0720200)	1	22	991	1011	.:: :::: ::::::::::	Translation	5.0

https://doi.org/10.1017/S0031182025000423 Published online by Cambridge University Press

Figure 1. Isolation and characterization of plasma EVs. (1A) Schematic overview of experimental methods. (1B) Transmission electron microscopy. (1C) Western blot detection of EXP-2, GAPDH, CD9, ApoB, and Cytochrome C1 (CYC1). (1D) Mode size and (1E) concentration between patients and uninfected individuals, compared using the unpaired 2-tailed t-test. Data are presented as mean values with SEM. (1F) Size distribution of extracellular particles [nm] versus concentration (particles/ml) (*P <0.05, **** P < 0.0001).

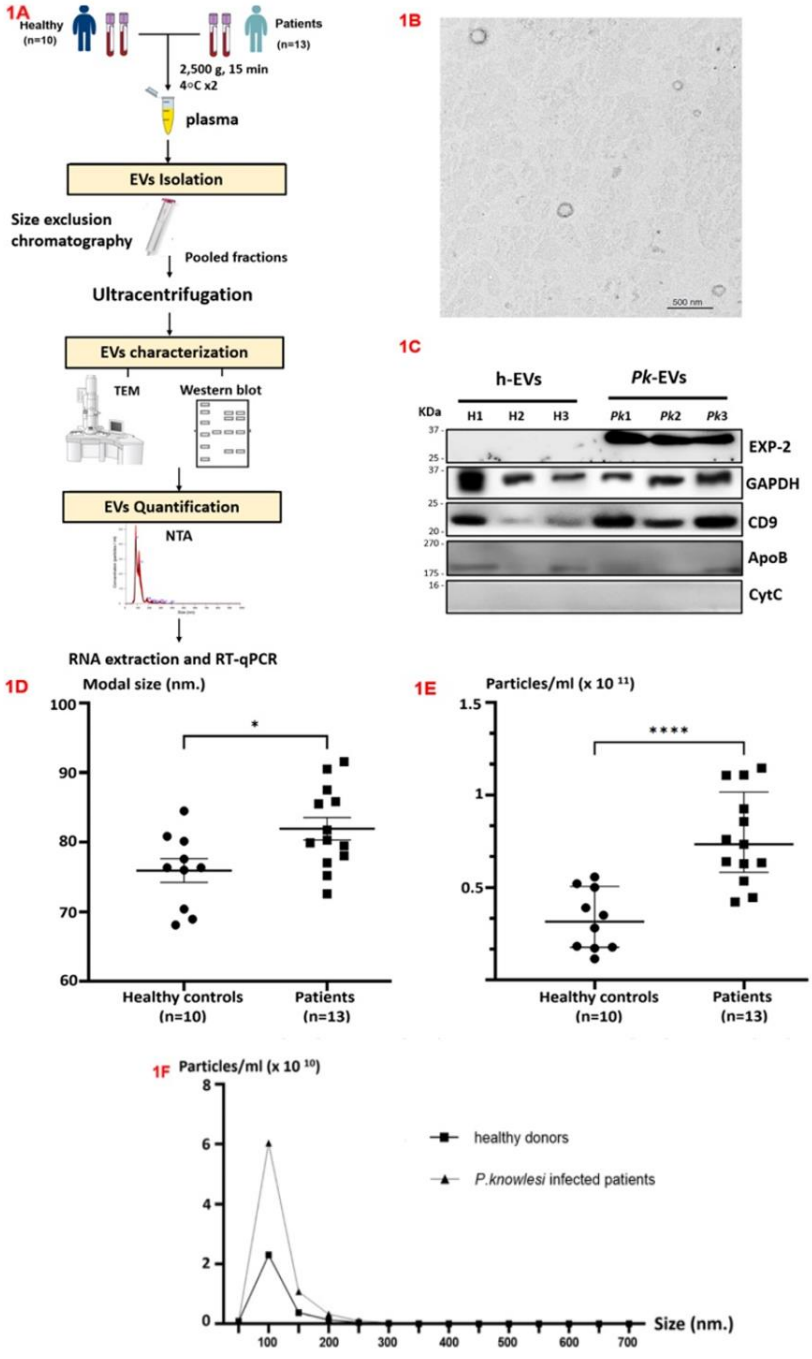

https://doi.org/10.1017/S0031182025000423 Published online by Cambridge University Press

Figure 2. Dot plots of miRNA relative expression in EVs derived from healthy controls and *P. knowlesi* infected individuals. Graphs display mean levels with SEM. Differences between the two groups were assessed by using the non-parametric Mann-Whitney U test (*$P < 0.05$,*** $P < 0.001$).

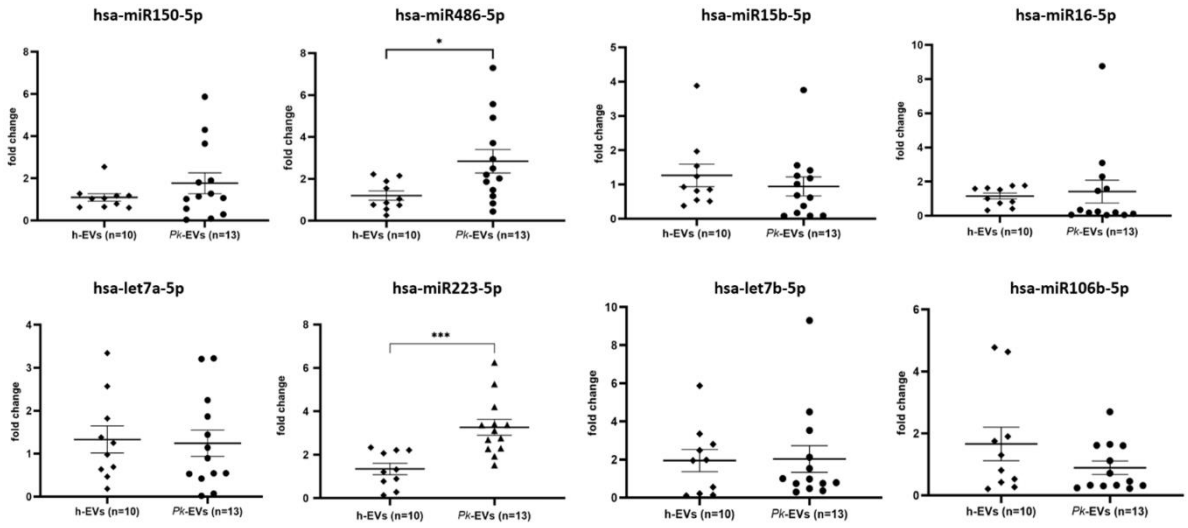

https://doi.org/10.1017/S0031182025000423 Published online by Cambridge University Press

Figure 3. Gene ontology (GO) and KEGG enrichment analysis of hsa-miR-223-5p and hsa-miR-486-5p. (A) Enriched GO terms of hsa-miR-486-5p performed using DIANA-miRPath. (B) Top 10 enriched GO terms associated with the predicted target genes of hsa-miR-223-5p, and (C) Top 10 enriched KEGG pathway associated with the predicted target genes of hsa-miR-223-5p. BP, biological process; CC, cellular component; DAVID, Database for Annotation, Visualization, and Integrated Discovery.

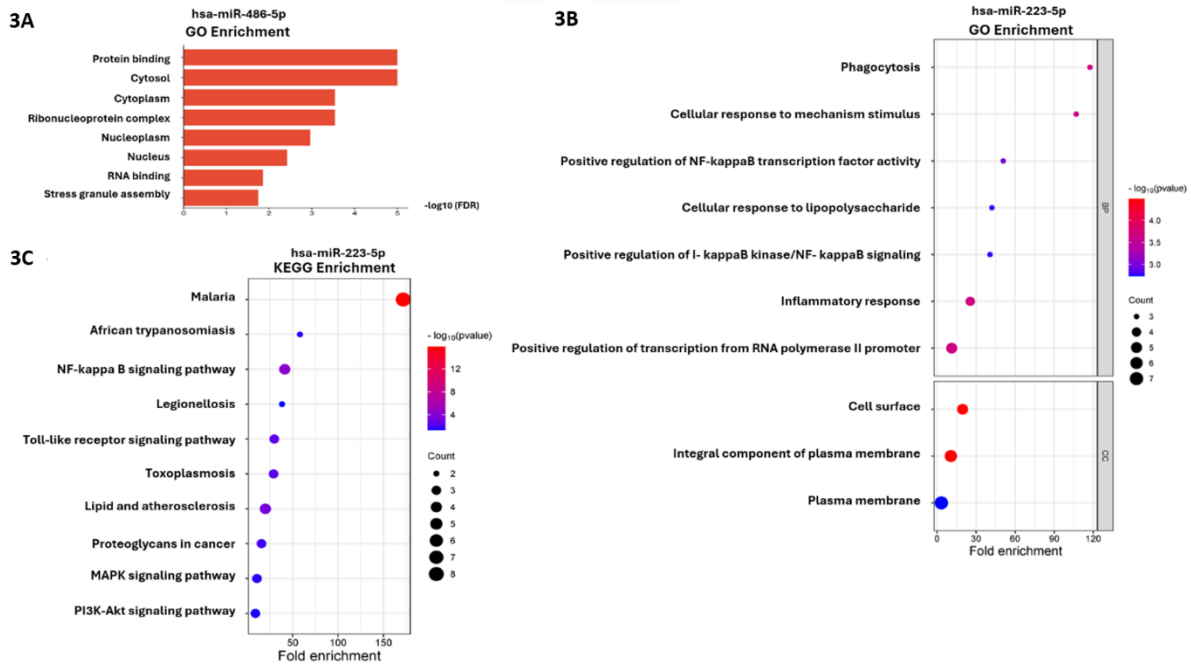

https://doi.org/10.1017/S0031182025000423 Published online by Cambridge University Press

Figure 4. Area under the ROC curve for miRNAs based on the RT-qPCR data. (A) hsa-miRNA-223-5p, and (B) hsa-miRNA-486-5p.

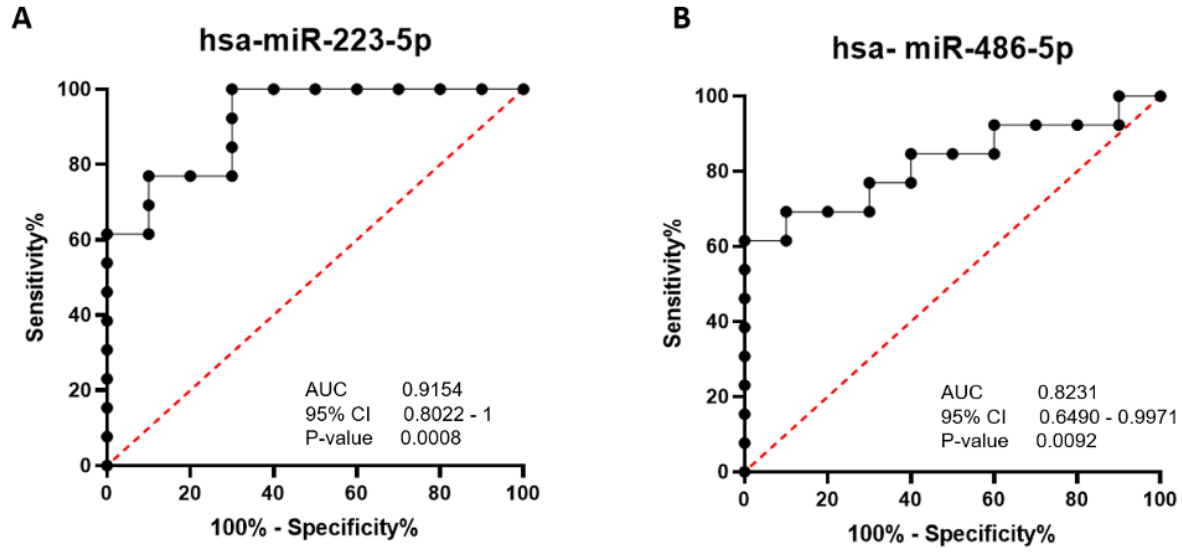

Graphical Abstracts:

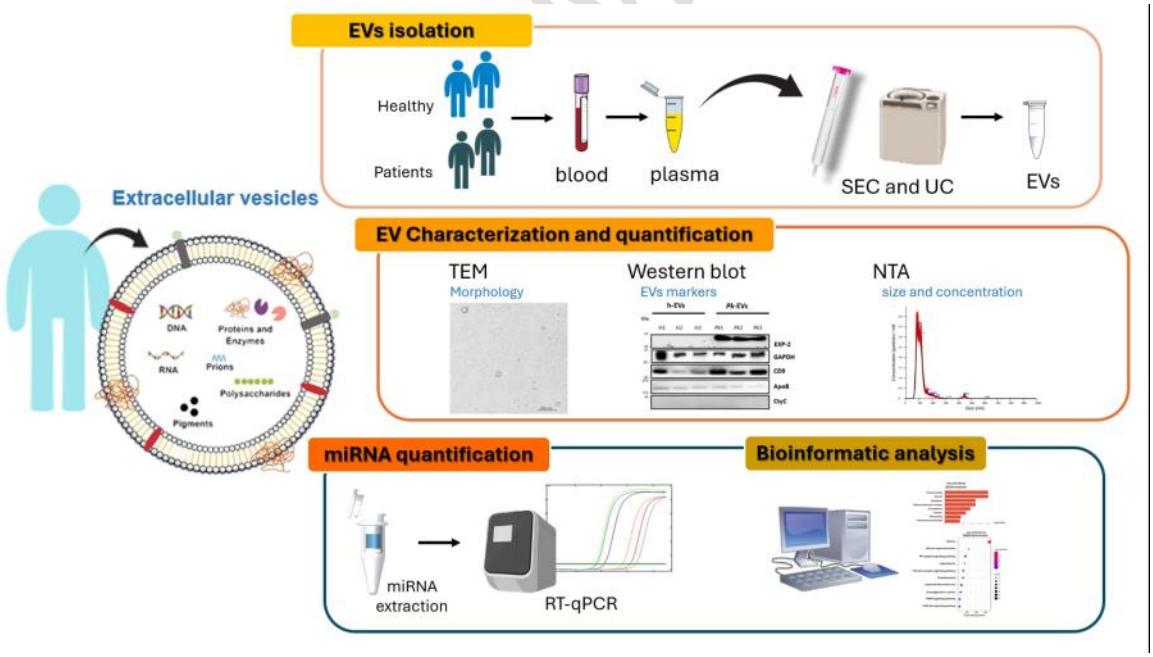

https://doi.org/10.1017/S0031182025000423 Published online by Cambridge University Press